Available online at www.sciencedirect.com
ScienceDirect
Polymer 48 (2007) 1679–1687
polymer
www.elsevier.com/locate/polymer

Detection of functional states of molecularly imprinted thin films with multi-cycling nanoindentation

Joseph J. BelBruno [a,*], Asta Richter [b], Sara E. Campbell [a], Ursula J. Gibson [c]

[a] Center for Nanomaterials Research, Department of Chemistry, Dartmouth College, Hanover, NH 03755 USA
[b] Department of Engineering Physics, University of Applied Sciences Wildau, 15745 Wildau, Germany
[c] Center for Nanomaterials Research, Thayer School of Engineering, Dartmouth College, Hanover, NH 03755 USA

Received 20 October 2006; received in revised form 21 November 2006; accepted 22 November 2006
Available online 15 February 2007

Abstract

Molecular imprinting is a chemical technique for the production of molecule-specific cavities. Spin casting with amino acids, aromatic molecules, carbohydrates or pesticides used as template molecules produces thin, selectively imprinted films of nylon-6 and other polymers. The film recognition activity is clearly coordinated with the appearance of nanometer-sized pores. The mechanical properties of the imprinted network reflect the various functional states of molecularly imprinted polymer films. Three specific functional states of the MIP were observed. Pores filled by template molecules may be distinguished from empty pores due to the variation in the elasticity modulus, the viscoelasticity and the hardness. The presence of the template molecule makes the polymer matrix stiffer due to strong hydrogen bonds (or other interactions) with the polymer chains. Films with empty pores have a higher viscoelasticity than those with filled pores. Changes in the polymer network are directly related to the nanomechanical properties and systematically studied in this work.

Keywords: Molecularly imprinted polymers; AFM; Nanoindentation

1. Introduction

Depth sensing indentation [1–3] is becoming a popular technique to measure the mechanical properties of nanometer-deep thin films. Load and penetration depth are simultaneously recorded during both loading and unloading. Hardness may be size-dependent, that is, hardness at small indentation depth is often greater than at large depths [1,2,4]. Polymers present a special problem, since their viscoelasticity may introduce complications into the typical analysis used in nanoindentation experiments. The current literature for nanoindentation in polymers [5–17] concentrates on extensions of current evaluation models and the development of proper measuring procedures, including time effects. An overview of the polymer indentation process, including details such as machine compliance, the use of different tip shapes and indenter systems is given in Ref. [5].

The standard Oliver–Pharr model [3] does not take into account the creep effects that may be present in materials with a time-dependent response, such as polymers and biological tissue. For example, the unloading curve in viscoelastic materials may have a negative slope if a small unloading rate and a relatively high load are used. Investigations of standard polymers, such as PMMA, have been reported using ramp loading and step loading histories to measure creep compliance [8]. Using either a Berkovich or spherical indenter, the time-dependent response under certain loading conditions for a linearly viscoelastic material was analyzed. Recently, amorphous polymers were investigated using variations in total penetration depth and unloading rates [14]. The elastic modulus was found to correlate strongly with the unloading strain rate, whereas its correlation with the indentation depth was statistically not significant.

* Corresponding author. Tel.: +1 603 646 2270; fax: +1 603 646 3946.
E-mail address: jjbchem@dartmouth.edu (J.J. BelBruno).

0032-3861/$ - see front matter © 2006 Elsevier Ltd. All rights reserved.
doi:10.1016/j.polymer.2006.11.054

Multi-cycling indentation combines quasi-static features with relatively slow repetition cycles and has been reported for investigations of mechanical properties in metals and semiconductors [4,18,19]. Depth dependent properties can be obtained using an effective time regime and, in such cases, pressure induced phase transformations are characterized by hysteresis loops. This method is ideally suited to the study of polymer materials and some initial reports have appeared [9,11,17]. If the unloading curve is not purely elastic, such as for polymer systems, hysteresis loops appear reflecting the viscoelastic energy loss. We have described a more detailed analysis of the load–time concepts used in multi-cycling indentation in thin nylon films in a previous paper [20].

Molecular imprinting of polymers is a chemical technique for the production of molecule-specific cavities that mimic the behavior of natural receptor binding sites, but may be created for any target molecule [21–29]. The concept is outlined in Fig. 1 and briefly described here. In the most general form, MIPs are prepared from the appropriate monomers in the presence of a template molecule that "binds" to the network via covalent, hydrogen bonding or other weak interactions. After polymerization, the template is removed and the polymer exhibits the ability to recognize the template with a high degree of selectivity. The figure shows these two states of a generic MIP. Typically, the MIP prepared according to the general procedure involves polymerization of a methacrylate monomer with photoinitiators in the presence of the template. The MIPs described here employ a crystalline polymer with a suitable theta solvent to eliminate the polymerization step. The MIP is created by dissolving the polymer in the presence of the template, allowing the new network to form in solution and, then, precipitating the MIP or casting it as a film. When dissolved the crystalline polymer is separated into elongated chains and the template molecules form bridges between the polymer chains. Evaporation of the solvent during spin coating produces the film.

Thin, selectively imprinted films of nylon-6 and other polymers are produced by spin casting with amino acids, aromatic molecules, carbohydrates or pesticides used as template molecules [25–28]. The film recognition activity is clearly coordinated with the appearance of nanometer-sized pores both on the surface and within the film [28]. Changes in the polymer network due to the polymer content in the spin coating process or the inclusion of different template molecules are directly causative to variations in the nanomechanical properties and are systematically studied in this work. The nanomechanical properties of the imprinted network reflect the various functional states of molecularly imprinted polymer films. Three specific functional states of the imprinted polymer were observed: as-produced films (with template still incorporated in the network), extracted films (template has been chemically removed, but the binding site remains) and reinserted template (again, by chemical means). In addition, the properties of a control film (template never included) serve to distinguish it from the three states of the functionalized films. Changes in indentation modulus, hardness and viscoelastic energy loss may be used to distinguish quickly among these different functionalized states. The aim of our investigations here is to develop a proper measuring procedure that accounts for the internal relaxation time of the imprinted films, the properties of the functionalized state and the rationale for the observations.

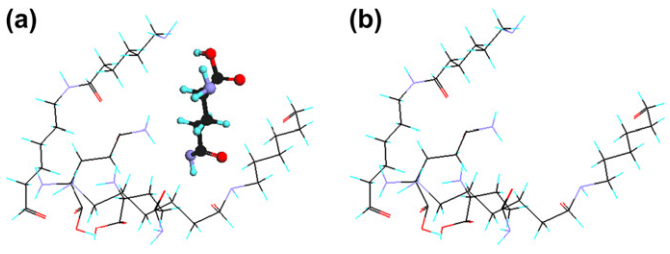

Fig. 1. Schematic of the procedure used to produce the imprinted polymer (here, nylon-6 and glutamine). Films with the template embedded (a) and the template removed (b). The polymer is shown as a backbone and the template molecule as a ball and stick model. Atom code: dark blue = nitrogen, red = oxygen, black = carbon and blue = hydrogen.

2. Experimental

Polymer films are produced from solutions that are 10% by weight solid polymer. Molecularly imprinted polymer (MIP) solutions contain 5–10% template molecule in addition to the polymer. The solvent is chosen so that both polymer and template are readily dissolved. For example, formic acid is employed for the nylon/amino acid system and methylethyl ketone/toluene for the Saran®/nitrobenzoate system. A complete list of polymers and templates used in these nanoindentation experiments is shown in Table 1. Thin films are produced using spin coating technology. Spin coating is a simple deposition technique sensitive to the composition and viscosity of the solution and the rotating speed of the plate. Our films were spin cast onto 18 mm square glass microscope cover slips that were pre-washed in concentrated nitric acid and cleaned with spectroscopic grade isopropanol and acetone prior to polymer deposition. The coating solution with the template embedded was dropped onto the spinning substrate and the spin coater was operated at speeds from 2000 to 9000 rpm for 30–60 s. The rotation spreads the solution evenly over the surface and causes the solvent to evaporate, leaving a thin film of material on the substrate. The substrate may be baked immediately after spin casting to remove any remaining solvent. Film thickness was measured using a Tencor Instruments Alpha Step 500 stylus profilometer and

Table 1
Summary of polymer/template systems employed in the MIP functional state analysis

MIP system number	Polymer	Template
1	Nylon-6	Glutamine
	Nylon-6	Alanine
	Nylon-6	Glycine
2	Poly-methylmethacrylate	Fructose
3	Saran® F-310	Methyl-4-nitrobenzoate
4	Polyvinylphenol	Fructose

a Micro-Xam Surface Mapping Microscope [25,26,28]. The concentration of polymer in the casting solution is the dominant variable for the film thickness, which increases with increasing polymer concentration. Samples with film thicknesses between 500 nm and 1.5 μm were used for the investigations reported in this paper. FTIR spectra were recorded over a narrow region of interest to confirm the chemical and functional nature of the polymer film [28]. Roughness measurements, R_a, were obtained by atomic force microscopy. The roughness varies with film components, but as typical values, the R_a of control nylon films and MIP films at scan size 30 μm × 30 μm is ~100 nm and 150–300 nm, respectively. The template can be removed by a proper choice of solvent to leave behind the cavity specific to the template molecule and may be subsequently reintroduced into the cavity.

All nanoindentation experiments were performed using the electrostatic transducer of the Hysitron triboscope in the UBI 1 [30]. The transducer consists of a three-plate capacitor, the mid-plate of which carries the impression tool fixed to a thin stylus. Application of a DC voltage generates an electrostatic force driving the indenter into the sample surface. Simultaneously the capacity change as a measure of penetration depth is recorded resulting in a force–depth curve. The stiffness of the internal springs holding the center plate needs to be measured and subtracted from the applied force in order to obtain the true sample stiffness. This electrostatic force constant (EFC) is calculated by performing an indentation in air, where the only resistance arises from the internal springs. The value of the EFC was checked several times during the experiments. Hardness, H, represents the mean contact pressure under load and is obtained by the applied load, F, divided by the projected area, A_c, of the indenter tip at the corresponding contact depth, h_c. The indentation modulus is derived from the slope of the force–displacement curve upon unloading as the material recovers elastically. The tip elastic properties can effectively be ignored for polymeric materials. Investigations are performed with a 90° diamond cube corner tip. The calibration of the tip to determine the depth dependent area function $A_c(h_c)$ was obtained with the standard curve-fitting method using fused quartz with its known reduced modulus as the reference material. Thermal drift and creep behavior of the piezoelectric scanner may affect the measurements and must be minimized. At the nanoscale, drift is measured and compensated for in the resulting data. This compensation factor in the standard UBI software is known as the drift correction [30]. This drift correction measurement is performed before each indent and its actual value is determined. Typical drift rates range up to 0.5 nm/s. In cases where the drift speed was larger, the indentation result was not used. The penetration depth of the indent should not exceed 30% of the polymer film thickness to avoid substrate effects. Most experiments have been performed with smaller penetration depths.

Depth dependent mechanical properties are obtained through indentation tests where repeated loading and unloading are performed at the same location on the sample surface [4,9,17,19] resulting in multi-cycling indents. In general, multi-cycling means, after loading to a maximum load, F_{max}, the sample is partially unloaded to a minimum force, $F_{min} = 0.1–0.25F_{max}$. This residual force is required to prevent the tip from losing contact with the sample and sliding to a new lateral position. The sample is then reloaded to the same or an increased maximum load ($F_{max} + \Delta F$) and the cycle is repeated. After the onset of plastic deformation (yielding), the loading curve is an overlap of both plastic and elastic deformations. If the unloading curve is not purely elastic, hysteresis loops appear which allow the analysis of viscoelastic properties. The analysis of the loops gives insight into the materials properties that change due to the applied contact pressure from the tip. Multi-cycling delivers a set of data that includes the entire material response, from the first indenter–sample contact to the maximum penetration.

3. Results and discussion

3.1. Nylon thin films

Before applying nanoindentation to imprinted films, it is important to demonstrate that all analysis techniques may be satisfactorily applied to a more characterized, but related material. A pure nylon film serves very well in this capacity and those used in the study were spin cast at 4500 rpm from 10% nylon (3 mm pellets with T_m 276 °C) in formic acid solution after stirring for 24 h. Single indent unloading curves for pure nylon (both semi-crystalline and amorphous) have a convex shape; an indication of viscoelasticity [1]. The bending of the unloading curve is more pronounced for slower loading rates or longer indentation times. As the time of the nanoindentation process is increased, the penetration of the tip into the material increases. Moreover, the requested maximum peak load is not attained; the nylon film is so soft and elastic that a large fraction of the applied load is used to stretch the spring that supports the center plate in the capacitor. The actual load on the sample varies between 60% and 70% of the setup load with loading rates between 1 μN/s and 100 μN/s. This indicates that the loading rate changes during the penetration process and is effectively diminished due to the measuring procedure. A loading function optimized to overcome this situation utilizes holding segments. The indentation depth is measured at peak load after holding. Variation in the holding time can be considered a creep test and gives valuable insight into the behavior of the material. If the holding time is sufficiently long (here, ~10 s), the slope in the graph changes, creep is diminished and saturation with respect to relaxation is reached. This holding time should be taken as an estimation of the point at which relaxation effects become less important and is the minimum holding time required.

Since the focus of this work is depth dependent nanomechanical properties, these lessons learned from the single indent experiments described above must be applied to multi-cycling processes as well. Fig. 2 presents the depth dependent nanohardness and indentation modulus data for a typical ~1 μm thick nylon film obtained with an optimized multi-cycling load function with holding segments [20]. The

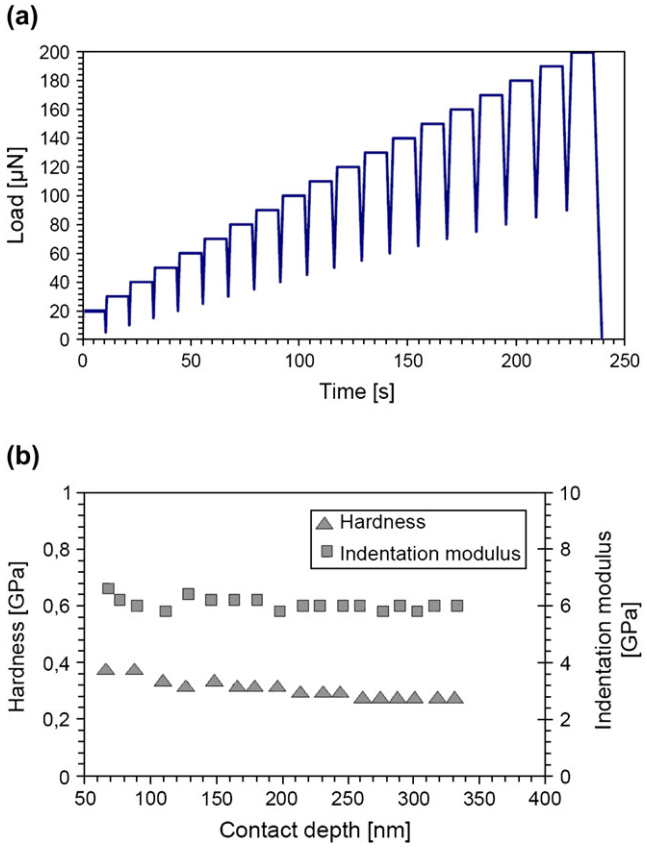

Fig. 2. Optimized multi-cycling load function with holding segments (a) and depth dependent hardness and indentation modulus for pure semi-crystalline nylon films (b).

nanohardness and indentation modulus are nearly depth independent and measured to be 0.31 (±0.06) GPa and 6.03 (±1.2) GPa, respectively. It is always necessary to check the polymer film without template molecule as a reference, since the morphology in the polymer matrix may change if the film changes from semi-crystalline to amorphous. Analysis of the hysteresis loops, obtained with an incrementally increasing five-cycle load function, indicates that the viscoelastic energy loss [9,17,20] is irreversible (increases with each cycle) and that the loss is greater in the amorphous material than in the semi-crystalline films. The relative energy loss is up to 50% in the former and approximately 33% in the latter. The behavior of the two types of nylon films may be rationalized in terms of a simple model. Adhesion energy is especially large when the polymer molecules are aligned, as they are in the solution used to cast the films and especially in the semi-crystalline films. The elastic behavior of the material under the indent is a result of the gliding of the aligned nylon chains after the adhesion energy between molecules has been overcome. Twisted nylon molecules are the basis for the observed viscoelastic effects. These chains are stretched by indentation and may either return to their original conformation or remain in a stretched state, as the indenter is unloaded. The hardness of amorphous and semi-crystalline nylon films does not differ too much, because of competing effects. The indentation modulus for semi-crystalline nylon films is remarkably larger and the viscoelastic energy loss is much smaller than that for amorphous nylon films.

3.2. Imprinted nylon films

Imprinted nylon films were produced as described above, but the solutions included 5% by weight of the imprint molecule, which in this case was an amino acid (glutamine, glycine or alanine). An example of the morphology of an alanine imprinted nylon film measured by atomic force microscopy (AFM) is shown in Fig. 3, alongside a control nylon film. Pure nylon films do not have pores, whereas all MIP films with any template molecule show characteristic pores. The size of the pores varies in dependence with the template molecule size and the extent of chemical interaction among template molecules and with host polymer molecules. Thus, the small alanine molecule results in pores with a diameter of about 285 nm and the glycine molecule has pores of ~850 nm size. Pore size in the nylon films is estimated to be ±25%. The morphology of the imprinted film does not significantly change when the template is extracted or subsequently reinserted. By means of infrared spectroscopy, three different functional states of the films could be assigned. The films could be as-produced (AP) in which the template molecule is still contained within the cavities of the film. The template could be removed (TR) typically by soaking for 30 s in a 5% aqueous acetic acid solution. The cavities remain but are now emptied of the original template. Finally, the template molecule could be reinserted (RE) by soaking for 2 min in a 5% aqueous formic acid solution that also contains 5% by weight of the template molecule.

While the AFM images show little differences among the three functional states of the imprinted films, significant variances in nanomechanical properties were recorded among the three states. The investigation of porous materials by nanoindentation is a challenge as recently reported [31,32] and was successfully applied to MIP films [17]. A summary of the results obtained in this work is shown in Table 2. For glutamine imprinted polymers, the change in functional state is reflected in the measured nanohardness, indentation modulus and the viscoelastic energy loss (see also Fig. 4). The original, AP films have a greater hardness and indentation modulus value than that of the control nylon film. After removal of the template molecule, the TR film exhibits a nanohardness and indentation modulus that are less than that of the control film. Reinsertion of the template, film RE, returns the hardness and the modulus values to those recorded for the AP films. The viscoelastic energy loss is largest for the softest film containing pores without the template molecules.

Data for alanine and glycine imprinted films are also contained in Table 2. The MIP AP films with alanine and glycine template molecules have the same hardness as the control nylon films. The indentation modulus for the alanine films with very small pores is larger than that for pure nylon films and the viscoelastic energy loss, 35%, is comparable to that of the nylon film, 37%. In the case of MIP films with glycine

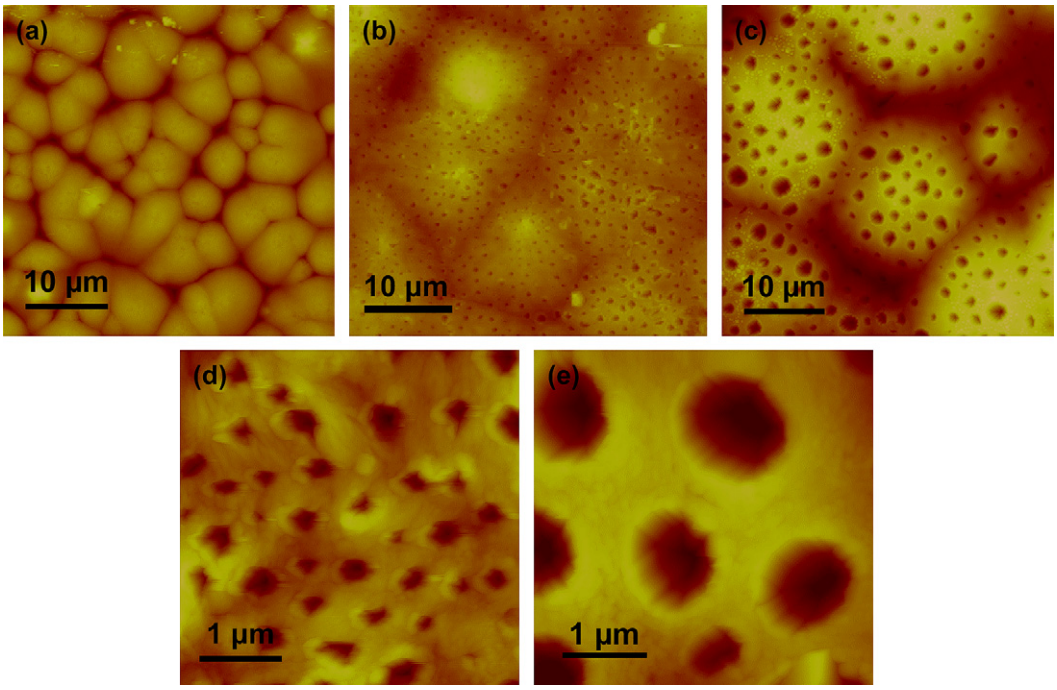

Fig. 3. AFM images of size 40 μm × 40 μm and height scale 1.5 μm for a pure control semi-crystalline nylon film (a), alanine-templated as-produced (AP) MIP film (b), glycine-templated AP MIP film (c) and AFM images of size 4 μm × 4 μm of alanine-templated (height scale 350 nm) (d) and glycine-templated AP MIP films (height scale 700 nm) (e).

template molecules, the AP film is much more elastic with a lower indentation modulus of 1.8 GPa and a higher viscoelastic energy loss of 40%. Removal of the template molecules in both MIP films results in a significant softening of the material indicated by a steep decrease in the hardness and the indentation modulus and a large increase in the viscoelastic energy loss. Reinserted template molecules make the material a bit stiffer, but it is still much softer than that of the AP films indicating that the reinsertion was not complete.

Computational modeling can provide a rationale for the relative behavior of the glutamine, glycine and alanine imprinted films. Here, the intent is to connect the nanohardness to a specific film structure. Previous work has reported on the two isomorphs of nylon-6: the α-phase that consists of a zigzag chain configuration and the γ-phase in which the chains are linearly aligned. The former is denser and this difference is reflected in higher measured bulk values for the hardness and Young's modulus [33,34]. For the imprinted polymer cases, there appears to be a correlation with the hydrogen bonding capability of the amino acid. The structure of glutamine lends itself to at least four possible hydrogen bonding sites (see Figs. 1a and 5a), while alanine and glycine exhibit, at most, two such sites (see Fig. 5b and c). One might simply assign the relative hardness to the number of hydrogen bonds between the template and the host polymer. This undoubtedly is a factor, however, in an attempt to define a more quantitative correlation, we have employed simple molecular modeling using a standard (universal force field) potential. While this type of calculation is not highly accurate for geometric and energetic parameters, the intent here is to define the basic differences among the possible MIP and control film structures using relatively inexpensive computational methods. Such calculations result in two different structures for the nylon-6 control polymer. In the control polymer calculations, a dimer of nylon-6 was used as the starting point, optimized and then additional nylon dimers were added to the system. Two different structures resulted, depending upon the structure of the initial dimer. If a linear chain was used, a calculation with up to six such dimers converged to a structure analogous to the nylon γ-phase. If the structure of the initial dimer was pre-optimized, resulting in bend at the sp^2 carbonyl carbon, a structure that resembles the zigzag geometry of the nylon α-phase was obtained. These simple tests provide confidence that the force field calculations are relevant to the experimental polymer

Table 2
Nanomechanical properties of control and amino acid imprinted nylon polymers

MIP system	Functional state	H (GPa)	E_r (GPa)	E_L (%)
Nylon control	–	0.20	2.2	37
Nylon/glutamine	AP	0.25	3.7	32
	TR	0.16	2.0	48
	RE	0.23	3.4	35
	RE with alanine	0.18	2.2	43
Nylon/alanine	AP	0.18	3.2	35
	TR	0.07	0.09	59
	RE	0.13	2.1	49
Nylon/glycine	AP	0.18	1.8	40
	TR	0.11	1.1	52
	RE	0.15	1.3	45

AP: as-produced film, TR: film with template removed, RE: film with template reinserted.

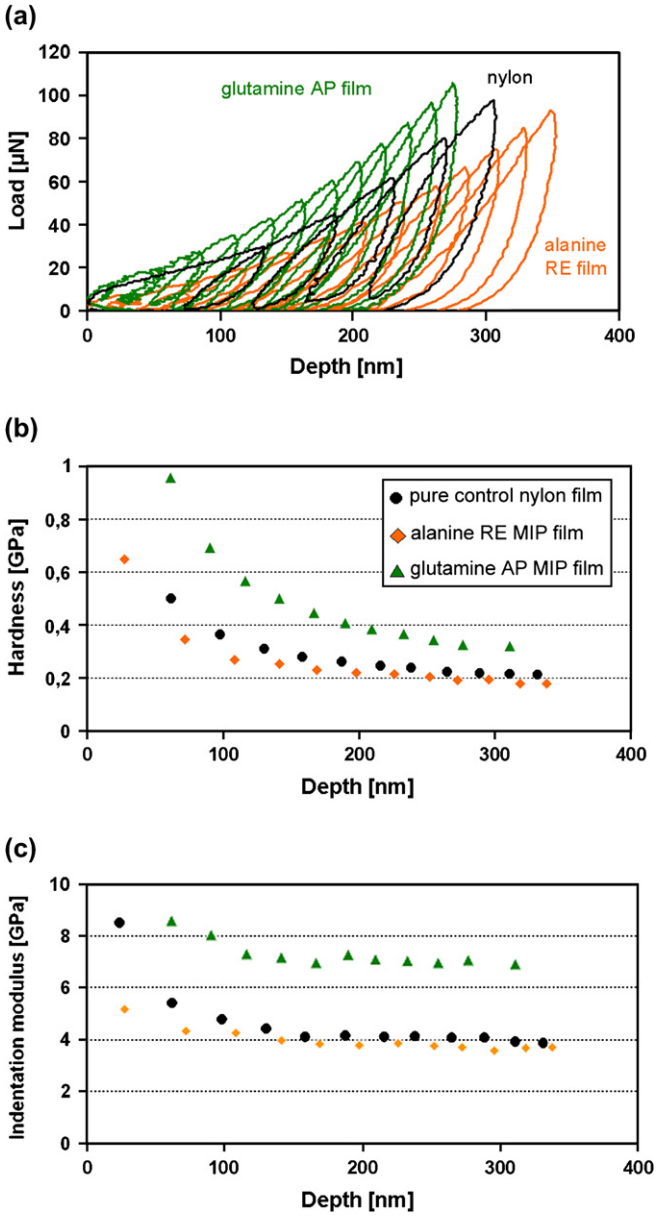

Fig. 4. Force–depth curves for a pure control nylon film, a glutamine-templated (AP) MIP film and an alanine reinserted template into the glutamine template removed MIP film (a) and the corresponding depth dependent hardness (b) and indentation modulus (c) for the three different functionalized MIP states.

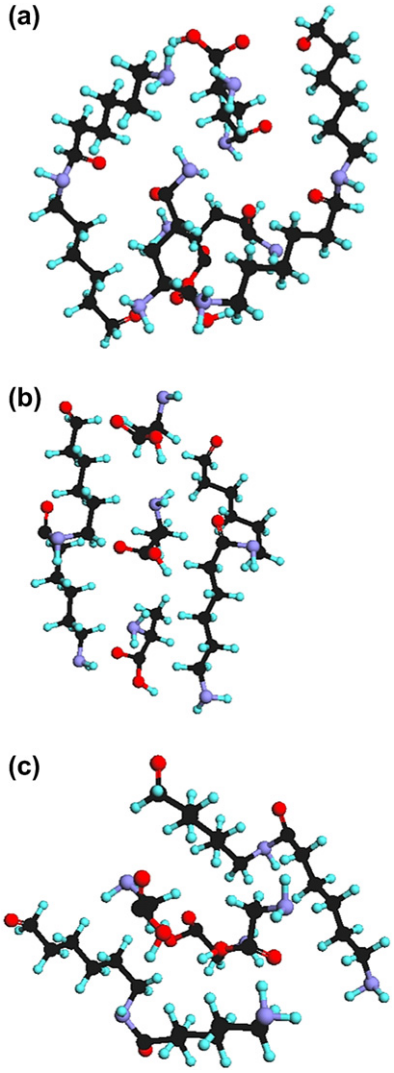

Fig. 5. Universal force field calculations for the structure of glutamine (a), alanine (b) or glycine (c) in a model nylon-6 host.

structure, at least in a qualitative sense. Fig. 5 presents views of analogous calculations for three different molecules, glutamine, alanine or glycine, in the presence of two nylon-6 dimers. Whether one begins with the linear or the bent nylon molecules described above, the same final geometries, those shown in the figure, are attained. In the modeling results, alanine is found to lie between the pair of nylon dimers arranged in a γ-like phase, effectively separating the linear-like nylon chains to a greater degree than in the control system (see Fig. 5b). One expects, therefore, that the presence of alanine as a template would reduce the hardness of the nylon host. This is exactly what has been observed in the nanoindentation experiments. The glycine–nylon MIP has a computed structure that locates the nylon chains in the α-like phase, but the nylon chains are more separated than that observed in the modeled alanine or glutamine MIPs (see Fig. 5a and c). Glycine appears to prefer another glycine as a hydrogen bonding partner, rather than a nylon molecule. This creates a softer film (in comparison to the control polymer or to the alanine-templated MIP) with larger than expected pores due to the clustering of the amino acid. Experimentally, one indeed observes a softer structure, since the indenter more easily passes through the large pored, more weakly hydrogen bonded MIP. In contrast to the alanine and glycine cases, the presence of glutamine has directed the nylon into a slightly helical (α-like phase) form with the amino acid packed relatively tightly into the cavity created by the host. Qualitatively, the density of this material would appear to be greater than that of the control sample and we expect and observe that the hardness increases relative to pure nylon-6.

The molecular cavities and micro-pores resulting from the imprinting process (see Fig. 3) change the mechanical

properties of a MIP with a glutamine template in two directions compared to pure nylon films: (1) filled cavities (a template loaded MIP) result in a small, but significant increase in hardness, a large increase in the indentation modulus and a small decrease in the viscoelastic energy loss. This represents a stiffer molecular network; and (2) empty cavities (extracted template molecules, but a polymer network still present) cause a large decrease in the hardness and the indentation modulus and a large increase in the viscoelastic energy loss. The empty MIP network can be easily squeezed together and results in a less stiff material in comparison to the pure nylon network. The chains are fixed by the polymer bonds, but the deformation around the cavity is flexible. Therefore, there is no gliding motion of the chains, but increased viscoelasticity (breathing cavities). The model and the process of employing nanomechanical properties to test the functional state of an imprinted polymer may be put to a test by attempting to insert a related template molecule, for example alanine, which is structurally similar, but smaller, into the glutamine-templated film. Here, the reinsertion process is applied as in the normal case, but after the process the slide is not washed with distilled water, as is normally done. Washing removes the alanine from the pores, as detected by infrared spectroscopy. This procedure results in a nanohardness that is only slightly larger than the TR nylon/glutamine film, as shown in Table 2 and Fig. 4. That comparison also indicates that the indentation modulus is slightly increased and the viscoelastic energy loss is a bit diminished. This result might be expected based on the model presented above. Alanine ''fits'' into the pores because it is smaller than the template, but it does not hydrogen bond to the nylon or, if it is coincidentally aligned with a nylon nitrogen or oxygen atom, it does not bond as strongly as the template glutamine molecule (see the results of the alanine-templated film in Table 2). This is reflected in the ease with which the indenter passes through the film. The MIP films with glycine as the template molecule also reflect the weaker hydrogen bonding with the nylon. Alanine and glycine are smaller molecular structures as compared with glutamine and this, too, contributes to the difference in stiffness. In the case of MIP films with glycine, all functionalized states are softer than the nylon control film as represented by a smaller hardness and a smaller indentation modulus and a large viscoelastic energy loss (see Table 2).

3.3. Saran® and imprinted polymers

Films have been produced from Saran® F-310, a copolymer of vinylidene chloride and methacrylonitrile. The solvent system for these films, methylethyl ketone and toluene, rapidly evaporates under most any spin coating conditions, leading to very thin films, typically of the order of 500 nm for casting from 10% template solutions. The template molecule is methyl-4-nitrobenzoate and the interaction between the template and host polymer is expected to occur via non-covalent interactions between the oxygen atoms in the template and the carbonyl groups within the polymer. *Preliminary* measurements, using a maximum force of 200 μN, indicate that the nanohardness of the control film is 0.15 GPa and is essentially independent of depth, but the control film indentation modulus decreases significantly, from 14 GPa to 10 GPa, over the indentation depth range of 60–170 nm. The templated polymer has a greater nanohardness, ~0.16–0.19 GPa, depending upon where in the film morphology the measurement is made. The template film indentation modulus varies in a fashion similar to the control film, with values from 14.5 GP to 9 GPa over the same indentation depth range. Early experiments focused on spectroscopic analysis to follow the production, extraction (in methanol) and reinsertion (10% benzoate in toluene) process for this film and the results indicated that the reinsertion process was not effective. The reason for this failure was unclear until the nanoindentation measurements were completed. The nanohardness of the RE polymer is significantly greater than that of either the control or the AP materials, 0.3 GPa at 110 nm. AFM images, Fig. 6, confirm that the reinsertion procedure thins the film by redissolving the polymer, leaving a material that is too thin to provide a suitable path length for optical measurements and thin enough so that the influence of the substrate is measured in the nanoindentation studies. Fig. 6 also indicates the changes in morphology for this system. The AP film, in Fig. 6a, shows crystalline regions (which may be the source of the depth dependent indentation modulus – the exact thickness of this region has not yet been determined), the RE film, Fig. 6b, thinned by the solvent has the templated pores visible and the TR film, in Fig. 6c, shows evidence of solvent damage where the film has been eroded down to the substrate. The greater hardness for the AP film, relative to the control film, results from the presence of the template–host polymer interactions, which are stronger than those within the host polymer itself. Most importantly, the ability of nanoindentation measurements to distinguish among the functional states is supported by these images and measurements.

3.4. Polyvinylphenol and imprinted polymers

Preliminary measurements have also been carried out on this polymer system, using a solution of 10% fructose (the template molecule) in methanol as the casting system. These films are 1–2 μm thick. Fig. 7 presents AFM images of the control and AP films. The morphologies shown in the figure are clearly functional state dependent. The control film is somewhat homogeneous and free of any cavities or pores. The AP film, on the other hand, has a membrane-like structure that is unique and results from the templating procedure with the sugar. This is reinforced by nanoindentation measurements. Both the nanohardness and the indentation modulus are independent of depth up to 400 nm. The control film has a nanohardness value of 0.3 GPa and E_r of 7 GPa, while the measurements for the templated, AP, film is 0.03 GPa and 1 GPa, respectively. The effect of the membrane-like structure on the nanomechanical properties is striking and a reflection of the cavities present in the AP film. The template has directed a complex structure that cannot be completely occupied by the fructose, leaving empty cavities that are easily indented in the measurement process. Again, the results confirm the

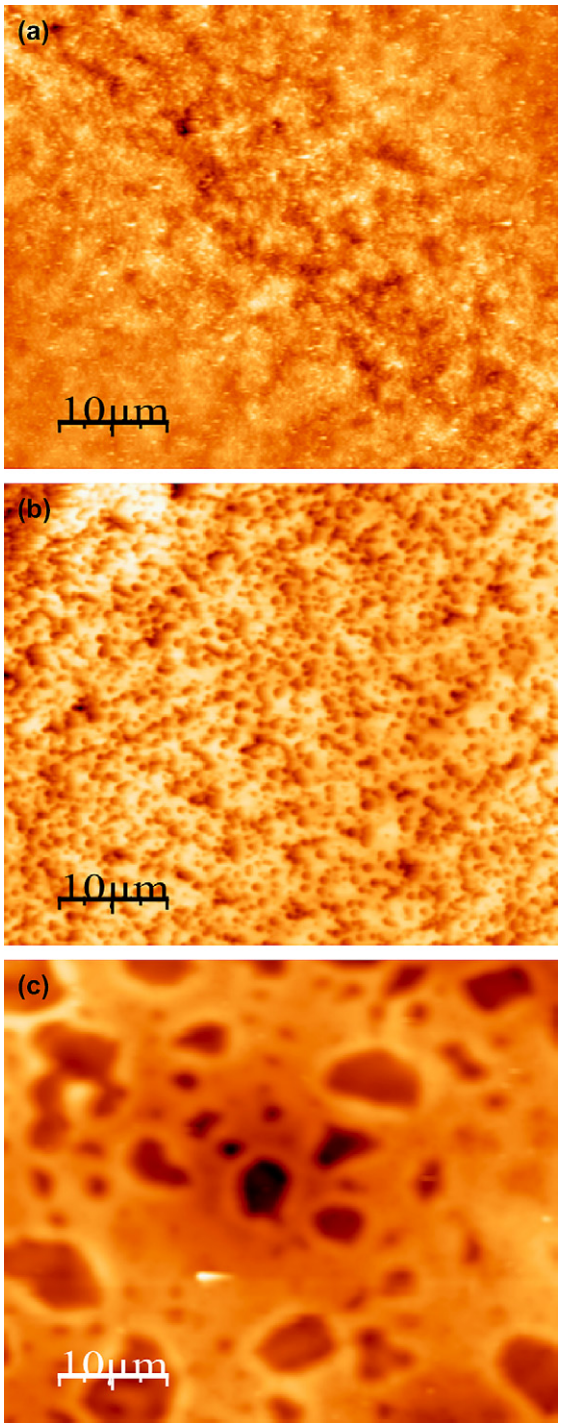

Fig. 6. AFM images of size 50 μm × 50 μm of the Saran®/nitrobenzoate system: control Saran® F-310 film (a), templated as-produced (b) and, template removed films (c).

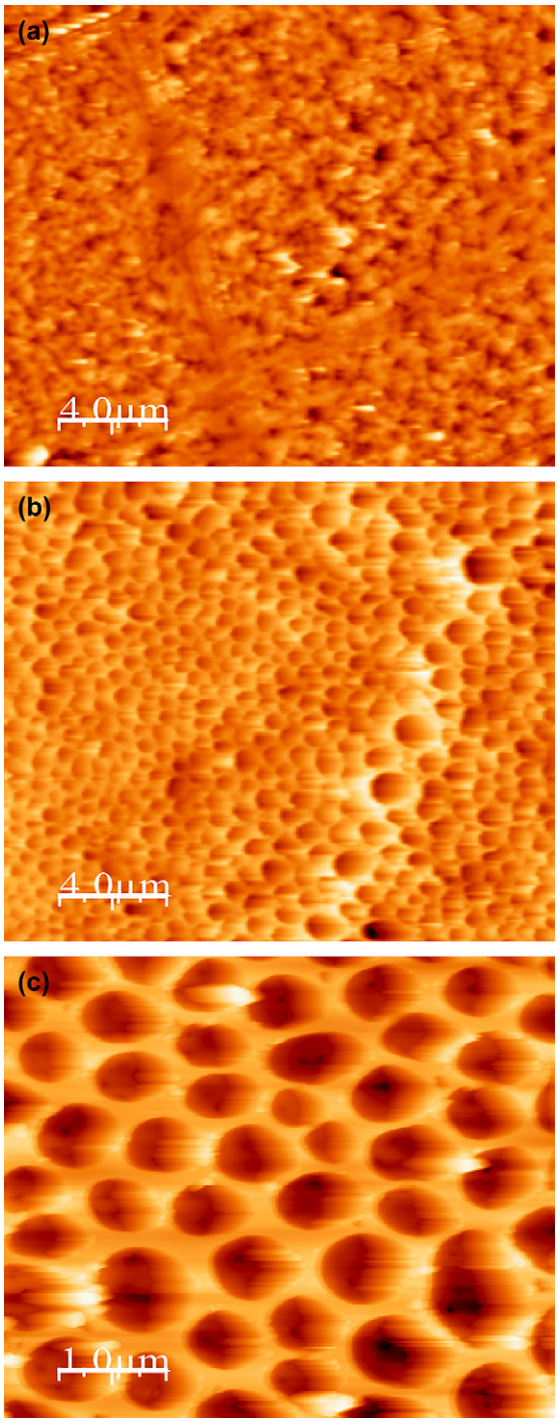

Fig. 7. AFM images of size 20 μm × 20 μm of the polyvinylphenol/fructose system: control polyvinylphenol (a) and templated as-produced films (b), a higher resolution, 5 μm × 5 μm, image of the AP film is also shown in (c).

ability of the hardness measurements to discern the functional state of the MIP.

4. Summary

We have described a procedure that employs multi-cycling nanoindentation to differentiate among functionalized states of molecularly imprinted polymer films. These interpretations are confirmed by spectroscopy and AFM images that indicate different morphologies for some of the states. In brief, we have shown that:

- MIP films show a typical surface morphology with a characteristic pore structure based on molecular cavities. The pores are larger than the template molecules, but specific

to the molecule based on both size and chemical interactions;
- the pores and the available bonding sites of the template within the polymer matrix modify the mechanical properties of the host polymer;
- the mechanical properties are different for the various functionalized MIP states corresponding to filled and empty pores. The functional states of the films may be distinguished by nanoindentation and
- computational modeling can provide a rationale for the relative behavior of different MIP systems and confirms the experimental results.

Acknowledgments

J.J.B. acknowledges the support of the National Science Foundation through grant INT-0233261 and the Cancer Nanotechnology Working Group at the Norris Cotton Cancer Center. A.R. gratefully acknowledges the sponsorship of the Harris German–Dartmouth Distinguished Visiting Professorship at Dartmouth College, during which part of this work was performed. We thank Charles P. Daghlian for support during the measurements at the Rippel Electron Microscope Facility Center at Dartmouth College.

References

[1] Fischer-Cripps AC. Nanoindentation. New York: Springer-Verlag; 2002.
[2] Bhushan B. Handbook of Nanotechnology. Heidelberg: Springer; 2004.
[3] Olivier WC, Pharr GM. J Mater Res 1992;7:1564–83.
[4] Wolf B, Richter A. New J Phys 2003;5:15.1–15.17.
[5] VanLandingham MR, Villarrubia JS, Guthrie WF, Meyers GF. Macromol Symp 2001;167:15–43.
[6] Klapperich C, Komvopoulos K, Pruitt L. J Tribol 2001;123:624–31.
[7] Feng G, Ngan AHW. J Mater Res 2002;17:660–8.
[8] Lu H, Wang B, Ma J, Huang G, Viswanathan H. Mech Time Depend Mater 2003;7:189–287.
[9] Nowicki M, Richter A, Wolf B, Kaczmarek H. Polymer 2003;44: 6599–606.
[10] Huang G, Wang B, Lu H. Mech Time Depend Mater 2004;8:345–64.
[11] Chang R-C, Huang B-C. Tamkang J Sci Eng 2005;8:217–24.
[12] Odegard GM, Gates TS, Herring HM. Exp Mech 2005;45:130–6.
[13] Clifford CA, Seah MP. Appl Surf Sci 2005;252:1915–33.
[14] Fujisawa N, Swain MV. J Mater Res 2006;21:708–14.
[15] Chakravartula A, Komvopoulos K. Appl Phys Lett 2006;88:131901.1–3.
[16] Tweedie CA, Van Vliet KJ. J Mater Res 2006;21:1576–89.
[17] Richter A, Gruner M, BelBruno JJ, Gibson UJ, Nowicki M. Colloids Surf A 2006;284–285:401–8.
[18] Domnich V, Gogotsi Y. Rev Adv Mater Sci 2002;3:1–36.
[19] Richter A, Wolf B, BelBruno J. Solid State Phenom 2004;95–96: 519–24.
[20] Richter A, Gojzewski H, BelBruno JJ. Int J Mater Res, in press.
[21] Alexander C, Anderson HS, Anderson LI, Ansell RJ, Kirsch N, Nicholls IA, et al. J Mol Recognit 2006;19:106–80.
[22] Yan HY, Row KH. Int J Mol Sci 2006;7:155–78.
[23] Yungerman I, Srebnik S. Chem Mater 2006;18:657–63.
[24] Matsui J, Sodeyama T, Tamaki K, Sugimoto N. Chem Commun 2006;30:3217–9.
[25] Shneshkoff N, Crabb K, BelBruno JJ. J Appl Polym Sci 2002;86: 3611–5.
[26] Maier P, Werner-Allen J, Gibson UJ, Richter A, BelBruno JJ. Surf Interface Anal 2004;36:1340–5.
[27] Schmidt RH, Mosbach K, Haupt K. Adv Mater 2004;16:719–22.
[28] Richter A, Gibson UJ, Nowicki M, BelBruno JJ. J Appl Polym Sci 2006;101:2919–26.
[29] Hayden O, Podlipna D, Chen X, Krassnig S, Leidl A, Dickert FL. Mater Sci Eng C 2006;26:924–8.
[30] Hysitron user handbook, feedback control users manual. 10025 Valley View Road, Minneapolis, MN 55344, USA; Hysitron Inc.
[31] Chen X, Xiang Y, Vlassek JJ. J Mater Res 2006;21:715–24.
[32] Gall K, Liu YP, Routkevitch D, Finch DS. J Eng Mater Technol 2006;128:225–33.
[33] Shen L, Phang IY, Liu T. Polym Test 2006;25:249–53.
[34] San SF, Wang ZC, Li SH, Liu JJ. Surf Coat Technol 2006;200: 5245–52.